J. Biochem. 2011;149(4):443–453 doi:10.1093/jb/mvq156

JB THE JOURNAL OF BIOCHEMISTRY

Different consequences of reactions with hydrogen peroxide and *t*-butyl hydroperoxide in the hyperoxidative inactivation of rat peroxiredoxin-4

Received November 22, 2010; accepted December 19, 2010; published online January 5, 2011

Yoshitaka Ikeda[1,*], Miyako Nakano[2], Hideyuki Ihara[1], Ritsu Ito[1], Naoyuki Taniguchi[2,3] and Junichi Fujii[4]

[1]Division of Molecular Cell Biology, Department of Biomolecular Sciences, Faculty of Medicine, Saga University, 5-1-1 Nabeshima, Saga 849-8501; [2]Department of Disease Glycomics, Institute of Scientific and Industrial Research, Osaka University, 2-1 Yamadaoka, Suita, Osaka 565-0871; [3]Systems Glycobiology Research Group, Advanced Research Institute, RIKEN, 2-1 Hirosawa, Wako, Saitama 351-0198; and [4]Department of Biochemistry and Molecular Biology, Graduate School of Medical Science, Yamagata University, 2-2-2 Iida-nishi, Yamagata 990-9585, Japan

*Yoshitaka Ikeda, Division of Molecular Cell Biology, Department of Biomolecular Sciences, Faculty of Medicine, Saga University, 5-1-1 Nabeshima, Saga 849-8501, Japan. Tel: +81 952 34 2190, Fax: +81 952 34 2189, email: yikeda@med.saga-u.ac.jp

Eukaryotic typical 2-Cys type peroxiredoxin (Prx) is inactivated by hyperoxidation of the peroxidatic cysteine to a sulphinic acid in a catalytic cycle-dependent manner. This inactivation process has been well documented for cytosolic isoforms of Prx. However, such a hyperoxidative inactivation has not fully been investigated in Prx-4, a secretable endoplasmic reticulum-resident isoform, in spite of being a typical 2-Cys type, and details of this process are reported herein. As has been observed in many peroxiredoxins, the peroxidase activity of Prx-4 was almost completely inhibited in the reaction with *t*-butyl hydroperoxide. On the other hand, when H_2O_2 was used as the substrate, the peroxidase activity significantly remained after oxidative damage. In spite of these different consequences, mass spectrometric analyses indicated that both reactions resulted in the same oxidative damage, i.e. sulphinic acid formation at the peroxidatic cysteine, suggesting that another cysteine in the active site confers the peroxidase activity. As suggested by the analyses using cysteine-substituted mutants sulphinic acid formation at the peroxidatic cysteine may play a role in the development of the possible alternative mechanism, thereby sustaining the peroxidase activity that prefers H_2O_2.

Keywords: ER/hyperoxidation/oxidative stress/peroxiredoxin/sulphinic acid.

Abbreviations: Prx, peroxiredoxin; *t*-BuOOH, t-butyl hydroperoxide; Trx, thioredoxin; TR, thioredoxin reductase; NADP, nicotinamide adenine dinucleotide phosphate; HPLC, high-performance liquid chromatography; LC, liquid chromatography; MS, mass spectrometry; ESI, electrospray ionization; PBS, phosphate-buffered saline; DTT, dithiothreitol; SDS–PAGE, sodium dodecyl sulphate-polyacrylamide gel electrophoresis; TFA, trifluoroacetic acid.

Peroxiredoxin (Prx) was initially identified as a protein with anti-oxidant properties that plays a role in protecting certain types of enzymes from inactivation via oxidation of thiol groups (*1*, *2*). Prx was reported to be a type of peroxidase, the activity of which is based on an electron supply by thioredoxin (*3–5*). In mammals, six isozymic forms are known for the Prx family of proteins: Prx-1 to 6 (*6*, *7*). Several studies have suggested that these proteins are involved in the detoxification of reactive oxygen species (ROS) and various diseases that are thought to be associated with the production of ROS and oxidative stress (*8–19*).

Among the six members in the mammalian Prx family, Prx-1 to 4 are known to be typical 2-Cys types, in which an interpeptidyl disulphide is formed by a reaction between the active-site cysteine residues of two subunits (*20*, *21*). In the catalytic cycle of the peroxidase activity of the 2-Cys-type Prx, the reaction of one cysteine, a peroxidatic cysteine, with a peroxide leads to the formation of a cysteine sulphenic acid. This unstable sulphenic acid form is subsequently allowed to react with the other catalytic cysteine, a resolving cysteine, thereby forming a disulphide in a homodimeric protein unit. The resulting oxidized enzyme is then reduced by the action of thioredoxin (Trx) and Trx reductase, with NADPH serving as the reducing agent.

In the catalytic cycle of 2-Cys type of Prx, when the sulphenic acid at the peroxidatic cysteine does not react with the other catalytic thiol but instead reacts with another molecule of the substrate peroxide, the resulting cysteine sulphenic acid is further oxidized to the corresponding sulphinic acid (*22–24*). This hyperoxidized form is relatively stable and resistant to attack by the resolving cysteine, thus leading to the inactivation of peroxidase activity. The irreversibly damaged enzyme can be revived by the action of a recently discovered protein, referred to as sulphiredoxin, in a glutathione- and ATP-dependent manner (*25–29*).

Inactivation as the result of hyperoxidation has been reported for several Prx forms, including Prx-4 (*23*, *24*, *30–34*). Because prokaryotic Prx is relatively resistant to hyperoxidation, it has been suggested that the mammalian enzymes may evolutionally adapt to act as a 'floodgate' that regulates the flow of H_2O_2 as an

intracellular signal (*35*, *36*). In fact, the structural motifs responsible for hyperoxidation have been identified in mammalian Prxs (*35*, *37*, *38*). In contrast to these isoforms that have been intensively studied, details of the inactivation process have not been investigated for Prx-4, and, because of this, it is not known whether the mammalian Prx isoform is inactivated in a manner similar to other typical 2-Cys-type Prxs. We recently successfully produced a mature form of rat Prx-4 using a baculovirus-insect cell expression system. Prx-4 contains a signal peptide which permits the protein to be targeted to the ER and then secreted into the extracellular space (*39*, *40*), and its domain organization consists of the signal peptide, a unique N-terminal extension and a family-homologous catalytic domain (*41*). Our improved expression strategy would permit the structural, enzymological and/or protein chemical bases of the actions and functions of this isoform of Prx to be examined in detail.

In this study, we report on an investigation of the process associated with the oxidative inactivation of Prx-4 that occurs in a catalytic cycle-dependent manner. The findings indicate that a significant level of peroxidase activity remains after inactivation by H_2O_2, while the activity is completely abolished in the case of a reaction with *t*-butyl hydroperoxide (*t*-BuOOH). Structural analyses using LC–MS indicated that both substrates give rise to the same oxidative damage, i.e. hyperoxidation of the peroxidatic cysteine residue. These results suggest that Prx-4 uniquely adapts to more preferentially detoxify H_2O_2, rather than being inactivated, as the result of the hyperoxidation.

Experimental Procedures

Cell culture and expression of the recombinant rat Prx-4 in insect cells

Spodoptera frugiperda (Sf) 21 cells were maintained at 27°C in Grace's insect media (GIBCO) supplemented with 10% foetal bovine serum, 3.33 g/l yeastolate, 3.33 g/l lactalbumin hydrolysate and 100 mg/l kanamycine. About 2×10^8 Sf21 cells, cultured in 20, 75 cm^2 flasks, were infected with a recombinant virus carrying a cDNA for rat Prx-4 (*39*, *42*) at a sufficient multiplicity of infection, and were harvested ~70 h post-infection for purification of the expressed protein.

Preparation of the recombinant rat Prx-4

Two truncated forms of recombinant rat Prx-4 that were expressed in the insect cells were purified as described previously (*41*). One form corresponds to a mature type, which is processed by cleavage of a signal peptide (*39*), and the other encompasses the domain equivalent to whole sequences of Prx-1 and Prx-2. The former and latter are designated as the 'mature form' and the 'catalytic domain', respectively. The harvested cells were rinsed with PBS and then centrifuged at 3,000 rpm for 5 min at room temperature. The precipitated cells were homogenized in 15 ml of 20 mM Tris–HCl, 1 mM EDTA, 5 mM DTT (pH 8.0) with a Dounce homogenizer. The homogenate was centrifuged at 15,000 rpm for 30 min, and the resulting supernatant was treated with 0.04% (v/v) polyethyleneimine to remove contaminating polynucleotides. After centrifugation, the clear supernatant was then dialysed against 31 of 20 mM Tris–HCl, 1 mM EDTA, 0.5 mM DTT (pH 8.0) at 4°C overnight with one change of the buffer. The dialysed sample was loaded on a DE52 column (bed volume, 10 ml) pre-equilibrated with the same buffer as the dialysis buffer. After washing the column with the buffer, the Prx-4 absorbed to the column was then eluted with a NaCl gradient from 0 to 0.5 M. The eluted Prx-4, the peak of which was detected by SDS–PAGE, was recovered and further purified on a Sephacryl S-200 gel filtration column (bed volume, 160 ml; 1.5 × 95 cm) using 20 mM Tris–HCl, 120 mM NaCl, 1 mM EDTA, 0.5 mM DTT (pH 7.5) as a solvent. The flow rate was 0.4–0.5 ml/min.

Electrophoresis

Proteins were subjected to SDS–PAGE analysis on 12.5% gels, according to Laemmli (*43*), and the protein bands were visualized by Coomassie brilliant blue R-250.

Assay for enzyme activity

The peroxidase activity of Prx-4 was measured by coupling with a Trx/Trx reductase system, essentially as described previously (*5*, *24*, *41*), and the reaction was spectrophotometrically monitored by the decrease in the absorbance of NADPH using a Beckman DU640 and a Hitachi U-2000 spectrophotometer. The standard assay was performed at 37°C with 0.5 mM H_2O_2 or *t*-BuOOH, 2.1 μM Trx (Promega), 50 nM Trx reductase (Sigma) and 0.2 mM NADPH in 0.1 M Hepes-NaOH (pH 7.0). The reaction was initiated by the addition of the enzyme or peroxides, and the oxidation of NADPH was continuously monitored at 340 nm. In some assays associated with curve fitting, the progress of the reaction was evaluated by calculating, using a molar extinction coefficient of 6.22 mM/cm at 340 nm. Amounts of product were estimated after subtracting the background based on the direct reduction of the peroxides by Trx. The purified enzymes were thoroughly reduced by incubation with 50 mM DTT at 37°C for 4 h, and the DTT was then removed by Sephadex G-25 gel filtration. This reducing procedure was performed immediately prior to all analyses in this study.

Hyperoxidation reactions and peptidase digestions of Prx-4 for the structural analyses

The exhaustively reduced Prx-4 catalytic domain (0.9 mg/ml, 200 μl of total volume) was incubated at 37°C for 40 min without or with 0.5 mM H_2O_2 or *t*-BuOOH in the presence of 2.1 μM Trx, 0.25 μM Trx reductase and 0.5 mM NADPH in 0.1 M Na-phosphate buffer and 1 mM EDTA (pH 7.0). When the peroxidase activities of the reacted enzymes were assayed using *t*-BuOOH, the activities were decreased to 5.6 and 0% in hyperoxidation reactions with H_2O_2 and *t*-BuOOH, respectively, as compared to the control, in which the enzyme was incubated without peroxide. The hyperoxidized enzymes were precipitated by 10% (w/v) of trichloroacetic acid on ice. After centrifugation, the pellets were rinsed with −20°C cooled acetone and dried in air. The dried pellets were dissolved in 67 μl of 8 M urea, 10 mM EDTA and 100 mM Tris–HCl (pH 8.0) and 3.5 μl of 34 mM freshly prepared iodoacetamide were added to each sample. The S-alkylation was allowed to proceed at 37°C for 30 min, and terminated by adding 3.5 μl of 80 mM 2-mercaptoethanol, 2.4 equivalent to the alkylating reagent. Digestion was then carried out at 37°C for 16 h with 1/180 the amount of lysylendopeptidase (Wako pure chemical).

LC–ESI–MS analyses of the peptides from t-BuOOH and H_2O_2-hyperoxidized Prx-4

The peptide mixtures were separated on an ODS column (Develosil 300ODS-HG-5, 150 × 1.0 mm, Nomura Chemical) using an acetonitrile gradient between 0 and 80% in 0.1% TFA. The gradient elution was performed for 80 min at a flow rate of 50 μl/min using an Agilent 1100 series HPLC system (Agilent Technologies). The eluate was continuously introduced into an electrospray ionization (ESI) source (Esquire HCT, Bruker Daltonics GmbsH). The proteins were identified using the NCBInr database with the MASCOT (Matrix Science) database-searching algorithm.

Protein determination

Protein contents were determined using a Bradford protein assay kit (Pierce), with bovine serum albumin was used as the standard.

Data analyses

Parameter calculations and data fitting were carried out by non-linear regression analyses using the computer software, SigmaPlot (Jandel Scientific) and Prism (GraphPad Software) for the Macintosh.

Results

Oxidative inactivation of Prx-4 by H_2O_2 and t-BuOOH

The catalytic cycle-dependent inactivation of Prx-4 was examined by incubating the mature form of the recombinant protein with hydrogen peroxide or *t*-BuOOH in the presence of Trx, Trx reductase and NADPH. The time course for the production of NADP did not show a constant increase in the reaction product, but downward curvatures were observed for both peroxides (Fig. 1A and B). Such a progressive decrease in peroxidase activity during the reaction is consistent with the hyperoxidation of an active site thiol, the peroxidatic cysteine (*24*), thus confirming that this isoform also undergoes oxidative inactivation during the catalytic cycle, as was reported previously in a proteomic study (*23*). As shown in Fig. 1A and B, the Trx system comprising Trx and Trx reductase solely catalyses NADPH-dependent reduction of peroxides. After adjusting for the background based on the direct reduction of peroxides by Trx and its reductase, however, the time courses for *t*-BuOOH and H_2O_2 showed quite different profiles (Fig. 1C). The enzyme activity was almost completely inhibited when *t*-BuOOH was used as the substrate, and thus only negligible amounts of NADP were produced after the initial inactivation process. In the case of H_2O_2, however, significant peroxidase activity remained, even after the inactivation process, as was also previously observed (*41*). The difference in the properties was more clearly explained by the derivative of the curve fitting (Fig. 1D), details of which are described below. Thus, the alteration of the enzyme by H_2O_2 appeared to involve the conversion of the enzyme into a less active form because the inactivated enzyme was subsequently able to produce NADP, albeit at a slower but constant rate, without further loss of the activity. Essentially the same results were obtained for another form encompassing the catalytic domain (data not shown), suggesting that such different properties in terms of inactivation are not associated with an N-terminal extension unique to Prx-4 but are intrinsic to the catalytic domain which corresponds to the overall structures of Prx-1 and Prx-2. Therefore, this form of the recombinant Prx-4 was used for further analyses in order to simplify the investigations.

Kinetic characterization of the inactivation processes by H_2O_2 and t-BuOOH

In order to characterize the inactivation processes by H_2O_2 and *t*-BuOOH in more detail, the time course for inactivation was further examined with various concentrations of peroxides. The reactions were continuously monitored spectrophotometrically, and the data, expressed as NADP production, were plotted at appropriate intervals as shown in Fig. 2A and B.

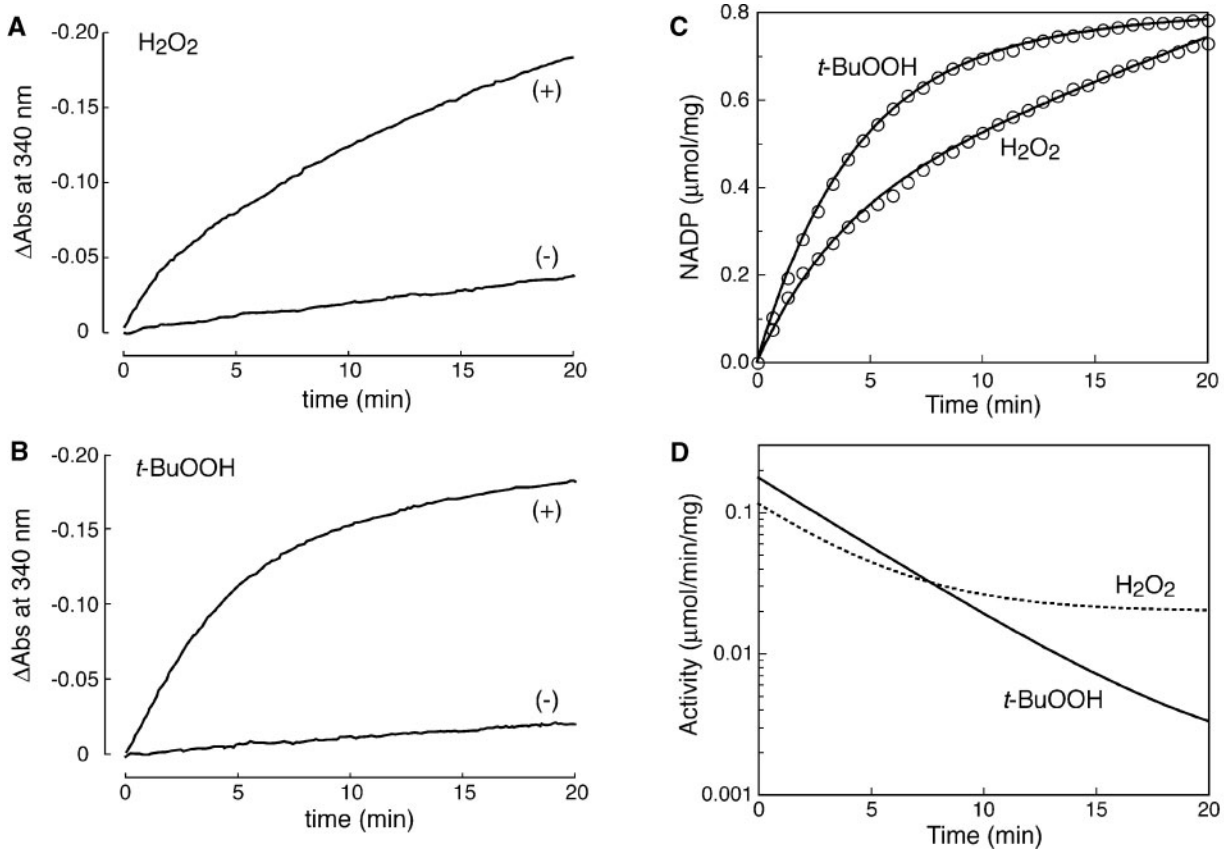

Fig. 1 Reactions of Prx-4 with H_2O_2 and *t*-BuOOH. (A and B) Recordings of NADPH oxidation for reactions with H_2O_2 and *t*-BuOOH. Changes in absorbance at 340 nm are shown for the presence (+) or absence (−) of 30 μg/ml of Prx-4. (C) Data calculated by subtracting the background are plotted as the NADP production at intervals of 40 s. Fitting curves are also shown for both reactions with H_2O_2 and *t*-BuOOH. (D) Derivatives of the fitting curves for reactions with H_2O_2 (dashed line) and *t*-BuOOH (solid line). Details are described in the text.

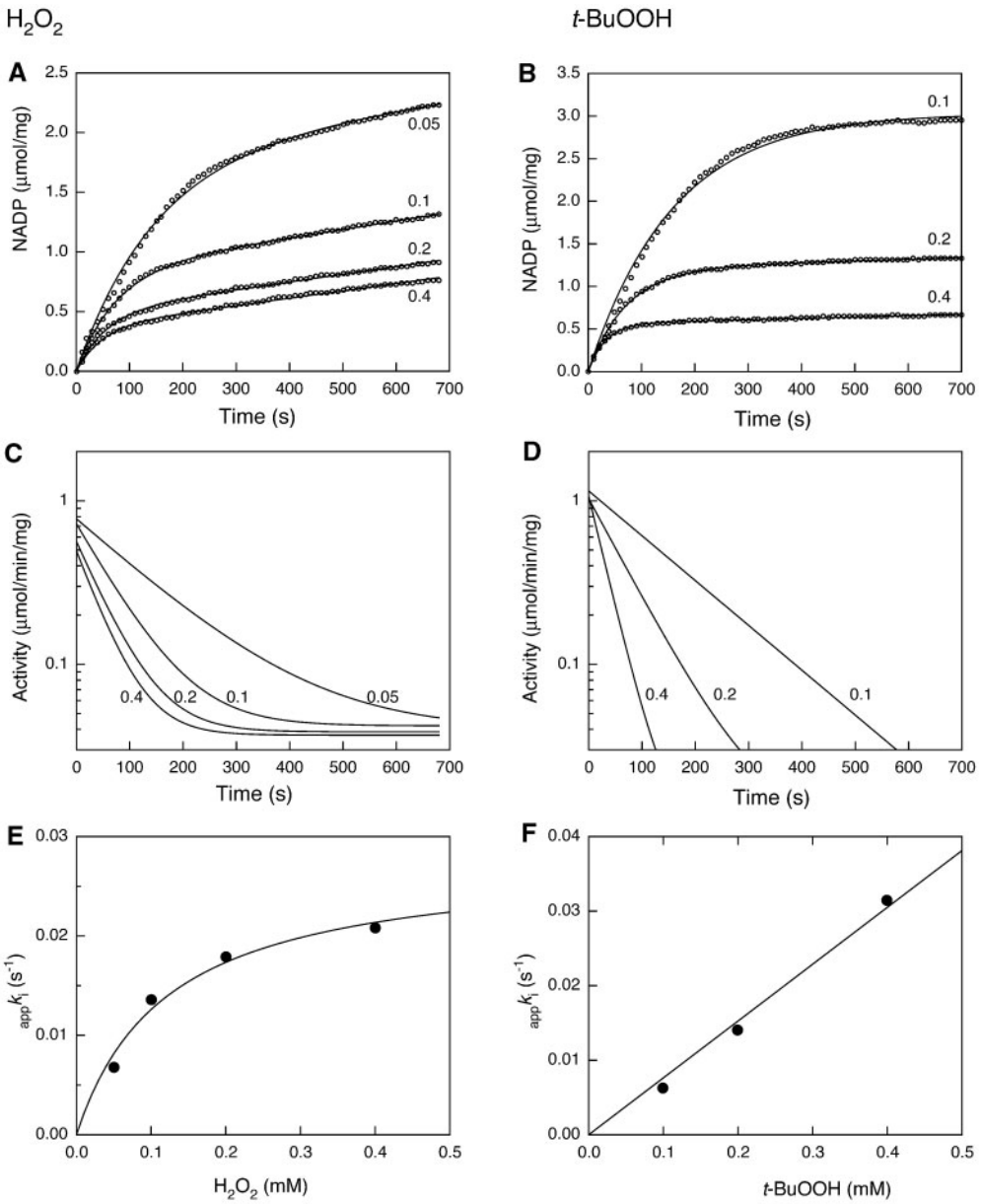

Fig. 2 Different kinetic profiles for the inhibition of Prx-4 by H_2O_2 and *t*-BuOOH. (A and B) Time course for NADP production calculated after subtracting the background. Data were obtained at intervals of 10 s are plotted and used for curve fitting using an equation described in the text. (C and D) Derivatives of the fitting curves for each data set for NADP production. (E and F) The parameter, $_{app}k_i$, which governs the rate of inactivation is re-plotted as the function of peroxide concentration. Details for the analyses are described in the text.

The data are presented after subtracting Prx-4-independent NADP production at each peroxide concentration, as carried out in Fig. 1. The direct reduction catalysed only by the Trx system displayed essentially the same linear increase of NADP at every concentration used (data not shown). As described in the 'Discussion' section and Fig. 7, because a small constant fraction of the active enzyme is inactivated by hyperoxidation in every catalytic cycle, a first-order exponential decay model may be used to fit the data for the sake of simplicity as follows:

$$v(t) = v_{act}\exp(-_{app}k_i t) + v_{inact}\{1 - \exp(-_{app}k_i t)\} \quad (1)$$

where, $v(t)$, v_{act} and v_{inact} are the overall reaction rate at time t and the reaction rates contributed by the initial active enzyme and by the inactivated enzyme species, respectively. The parameter, $_{app}k_i$, is an apparent pseudo-first order reaction constant that includes the concentration of the peroxide and controls the rate of inactivation. It should be noted that this parameter is the product of the actual rate constant for oxidation of a sulphenic form of the enzyme to a sulphinic acid derivative and a constant value for the fraction of the sulphenic enzyme species in the total active enzyme under steady state conditions. Thus, integration of Eq. 1 yields the product concentration at time t, which is expressed as

$$[P]_t = (v_{act}/_{app}k_i)\{1 - \exp(-_{app}k_i t)\} + (v_{inact}/_{app}k_i)\{\exp(-_{app}k_i t) - 1\} + v_{inact}t \quad (2)$$

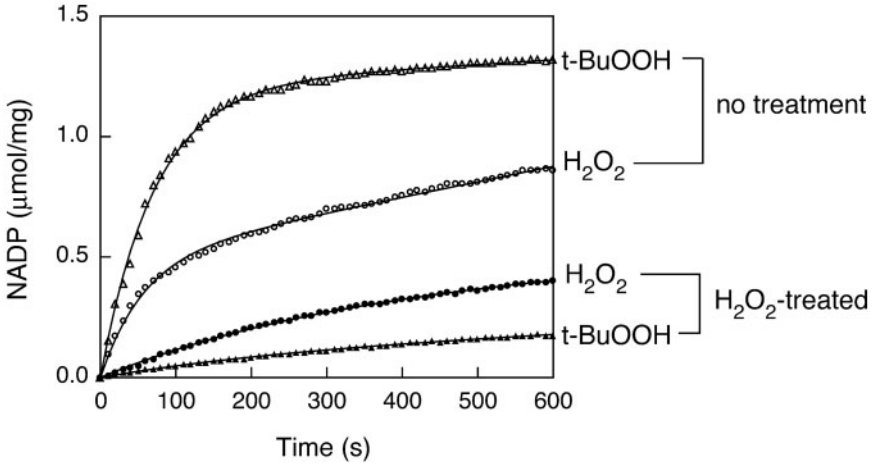

Fig. 3 Altered substrate preference in the H_2O_2-inactivated Prx-4. The reactions were carried out using 0.1 mM H_2O_2 and *t*-BuOOH.

As indicated in Fig. 2A and B, Eq. 2 is well fitted to the experimental data obtained for H_2O_2 and *t*-BuOOH, respectively. The first derivatives of the fittings, expressed as Eq. 1, are also shown in Fig. 2C and D using the parameters calculated. These kinetic analyses are consistent with a scenario in which the enzyme is 'converted' into an apparently low active species by reaction with H_2O_2 while the reaction with *t*-BuOOH results in complete inactivation.

Different inactivation kinetic profiles in the reactions with H_2O_2 and t-BuOOH

When the apparent first-order rate constant for inactivation, ${}_{app}k_i$, are plotted as a function of the concentration of the peroxide substrate, a linear relationship was found between [*t*-BuOOH] and the apparent rate constant (Fig. 2F). Thus, ${}_{app}k_i$ can be expressed using an apparent second order rate constant, k_i, as

$$ {}_{app}k_i = k_i\,[t\text{-BuOOH}] \qquad (3) $$

where, the quotient of k_i by the fraction of sulphenic species in the active enzyme, as described above, gives a parameter for the oxidation of the sulphenic acid form. As a result, the inactivation process in which the sulphenic acid species was further oxidized to the sulphinic acid form by *t*-BuOOH can apparently be regarded as a simple bimolecular reaction. The k_i value was calculated to be 75 M/s from the slope in Fig. 2F. As found in Fig. 2E, on the other hand, the catalytic cycle-dependent inactivation by H_2O_2 indicates simple saturation kinetics, similarly to a Michaelis–Menten model for the enzyme reaction, suggesting that the process of this inactivation involves the formation of a complex involving the sulphenic acid form of the enzyme and H_2O_2. By fitting the data to a simple saturation kinetic model

$$ {}_{app}k_i = k'_i\,[H_2O_2]/(K_i+[H_2O_2]) \qquad (4) $$

the apparent dissociation constant, K_i, equivalent to the Michaelis constant for the enzyme reaction, was calculated to be 0.12 mM, and a first order inactivation rate constant, k'_i, equivalent to the parameter such as k_{cat}, was 0.028/s. The K_i value appears to be much larger than Km values expected for peroxidase reactions of Prx-4 and other Prx isoforms (*44*). In fact, 0.05 mM H_2O_2 is a sufficiently saturating concentration for peroxidase activities, as indicated by a set of similar initial velocities shown in Fig. 2A. Therefore, these results suggest that H_2O_2 binds to the sulphenic acid enzyme species in a manner distinct from the case for the binding of the substrate to the intact free enzyme.

Characterization of the peroxidase activities of the H_2O_2-inactivated enzyme in comparison with the non-treated one

The recombinant Prx-4 was allowed to react with H_2O_2 in the presence of Trx, TR and NADPH until NADP was produced at a constant rate, where the inactivation was nearly completed, and low molecular compounds, including the peroxide, were then separated from the inactivated enzyme by Sephadex G50 column chromatography. The peroxidase activities of the resulting H_2O_2-treated enzyme were immediately re-assessed using both H_2O_2 and *t*-BuOOH as substrates. As shown in Fig. 3, the peroxidase activities of the treated enzyme were, as expected, lowered for both peroxide substrates, compared to the non-treated sample. This alteration was not reversed by treatment with DTT. The ratio of peroxidase activities, compared to the initial velocities, for H_2O_2 and *t*-BuOOH were determined to be 0.6 for the untreated and 2.1 for the H_2O_2-treated enzymes, respectively. As suggested by this inversion in the relative activities for these two peroxides the substrate preference for Prx-4 appeared to be altered, as the result of inactivation by H_2O_2. In addition, the enzymes were kinetically characterized under conditions of saturating *t*-BuOOH in order to examine alterations in kinetic properties with respect to Trx. As shown in Fig. 4, inactivation with H_2O_2 resulted in an increased Km for Trx by almost five times while the V_{max} value was decreased to as low as 5% of the control for the reaction with *t*-BuOOH as the substrate. Thus, when H_2O_2 is used as the substrate for the peroxidase activity of Prx-4, it appears likely

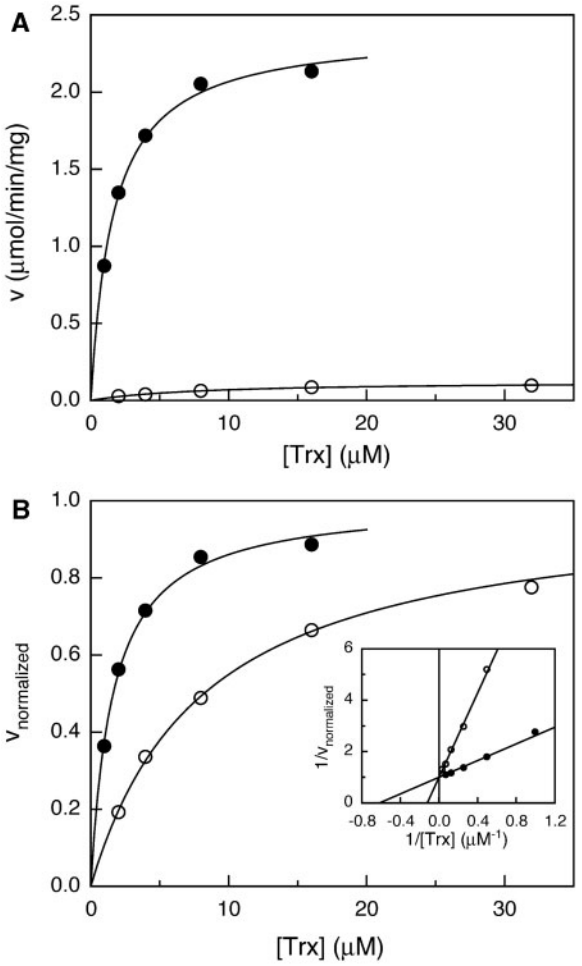

Fig. 4 Comparison of kinetic properties of intact and H_2O_2-inactivated enzymes with respect to Trx. (A) Reaction velocities plotted as the function of Trx concentration under saturating conditions of peroxide. Closed and open circles denote intact and H_2O_2-inactivated enzymes, respectively. (B) Data normalized by the maximal velocities calculated for each data set. Superimposed are double-reciprocal plots for the normalized data.

that the hyperoxidation process gives rise to an alteration of the enzymatic properties.

Structural analyses of the modification of Prx-4 in the catalytic cycle-dependent inactivation by H_2O_2 and t-BuOOH

After the reactions with H_2O_2 and *t*-BuOOH in the presence of Trx, TR and NADPH, the inactivated enzymes were separated on a Sephadex G-50 column to investigate the modifications that might underlie the different consequences. The isolated proteins as well as an untreated control sample were denatured by treatment with urea and then alkylated by reaction with iodoacetamide. These proteins were digested with lysylendopeptidase, and the resulting peptides were analysed by reversed phase HPLC and ESI-mass spectrometry (Fig. 5). The mass spectrometric analyses identified all of the cysteine-containing peptides in the chromatograms for the control, H_2O_2-treated and *t*-BuOOH-treated samples. Although the reactions with H_2O_2 and *t*-BuOOH exhibited different inactivation processes, the analyses indicated that these two peroxides caused identical oxidative modifications. In both the H_2O_2 and *t*-BuOOH-treated enzymes, only the formation of sulphinic acid at the peroxidatic cysteine residue was observed, as has been reported for other mammalian Prx isoforms (*22–24*, *26*, *31*), and no other significant modification was detected in the entire amino acid sequence. In fact, in all samples, the mass spectrometric analyses gave m/z values consistent with the presence of carbamidomethy-cysteine for the other two cysteine residues, a resolving cysteine, Cys-247 and a non-catalytic cysteine, Cys-150. A comparison of the HPLC profiles also indicated no other structural differences. A non-reducing SDS–PAGE analysis showed only a band corresponding to a monomer for the H_2O_2-hyperoxidized enzyme as well as *t*-BuOOH (data not shown), indicating the absence of disulphide formation. These results suggest that the other two cysteines remain free or reversibly oxidized thiols such as an unstable sulphenic acid might be formed during the peroxidase reaction of the hyperoxidized enzyme with H_2O_2. Thus, it is more likely that the enzyme decomposes the peroxides by an alternative mechanism that involves neither the peroxidatic cysteine nor disulphide formation.

Peroxidase activities of cysteine mutants of Prx-4

Mutant Prx-4 proteins in which cysteine residues were replaced with serine were prepared in order to determine whether cysteine residues, Cys-150 or Cys-247, as well as Cys-126 are involved in the reaction with H_2O_2, because a putative unusual catalytic cysteine residue might permit an alternative mechanism that does not primarily involve the peroxidatic cysteine to operate. As shown in Fig. 6A, a very weak activity was detected in the C247S mutant when *t*-BuOOH was used as the substrate. It appears that the C247S mutant functions as a peroxidase, possibly similar to a 1-Cys type Prx such as mammalian Prx-6, albeit the protein showed only marginal activity. However, because the C126S mutant did not exhibit a single catalytic turnover at all during the measurement up to 600 s (Fig. 6A), the mutant is quite inactive with respect to *t*-BuOOH, consistent with the result showing that the hyperoxidation of Cys-126 impairs the peroxidase activity toward *t*-BuOOH more severely. On the other hand, when H_2O_2 was used for the peroxidase assay of the mutants, activity was detected in both the C126S and C247S mutants (Fig. 6B). The C247S mutant exhibited a substantial Trx-dependent peroxidase activity, ~25%, compared to the wild-type and C150S in terms of its initial velocity. In comparisons of the initial velocity, the C126S mutant still retained nearly 10% of the activities of the wild-type and C150S. Moreover, it is noteworthy that the initial activity of C126S was quite comparable to the activities of the hyperoxidized forms of the wild-type and C150S, as evidenced by a comparison of the value at time 0 for the C126S and the values after ~600 s for the wild-type and the C150S (Fig. 6C). This concordance in velocities accounts for the functionality of Cys-247 as the alternative catalytic residue after inactivation by

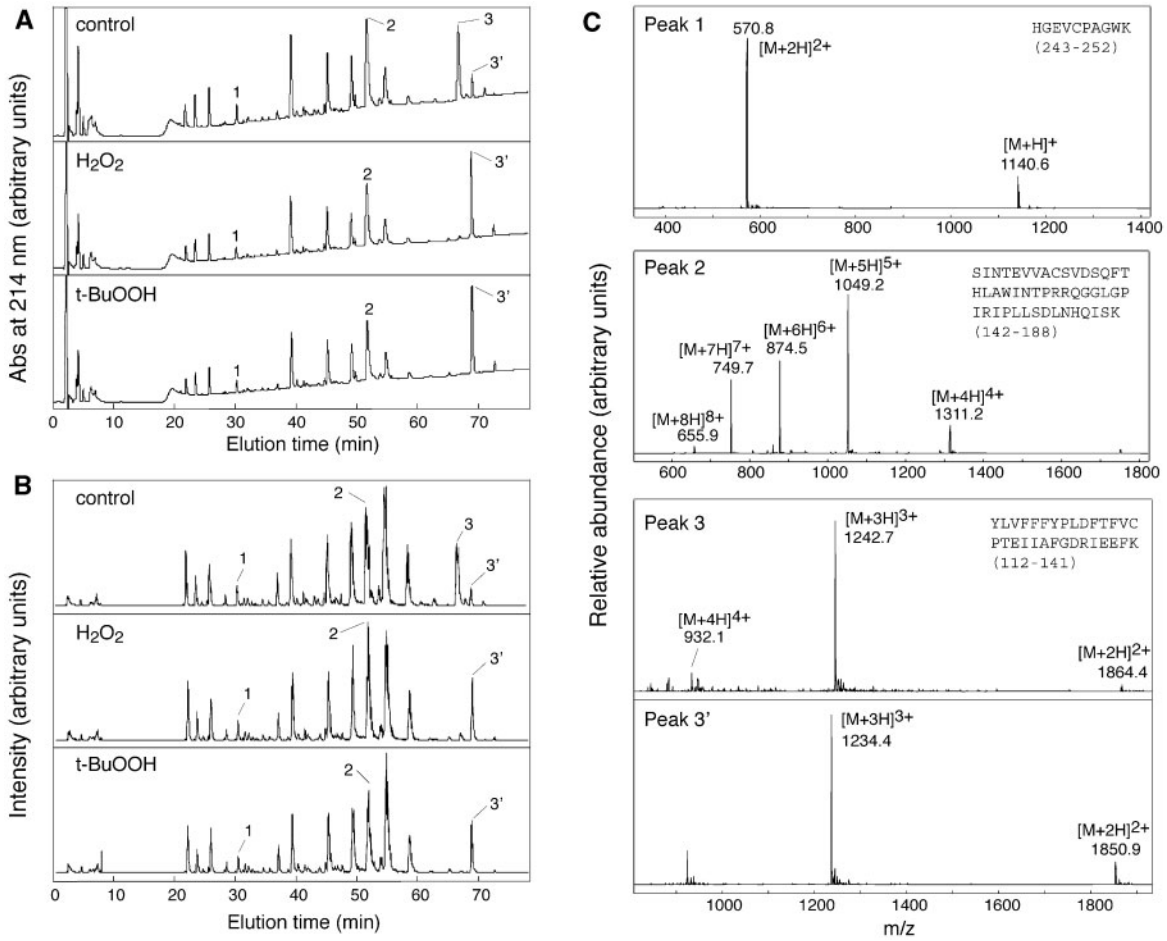

Fig. 5 Reversed phase HPLC and ESI–MS analyses of the modification by hyperoxidation in Prx-4. Lysylendopeptidase digestions of untreated, H_2O_2-inactivated and *t*-BuOOH-inactivated enzymes were analysed by reversed phase HPLC. The elution profiles of the peptides were monitored by absorbance at 214 nm (A) and also by on-line MS, given as base peak chromatograms (B). Numbers in these elution profiles indicate the peptide peaks that contain cysteine residues. Representative results for ESI–MS analyses of cysteine-containing peptides are shown along with the corresponding peptide sequences (C). All MS analyses for each peak gave quite the same m/z values, and indicate that the peptides contain carbamidomethyl-cysteine residues for peaks 1, 2 and 3, consistent with the alkylation by iodoacetamide and therefore with the absence of oxidation of cysteine. However, the MS analysis of peak 3′ shows that the peptide contained the hyperoxidized form of Cys-126 that had been converted into a sulphinic acid.

the hyperoxidation of Cys-126 to a sulphinic acid. However, while the wild-type and the C150S enzymes displayed no further inactivation after the hyperoxidation of Cys-126, the C126S mutant was smoothly inactivated following pseudo-first-order kinetics and completely lost most of its activity after two rounds of the catalytic cycle. If it is assumed that a putative sulphenic acid intermediate of the Cys-247 in the C126S mutant is partitioned into entering the next catalytic cycle with the concomitant oxidation of NADPH and otherwise being hyperoxidized, the total product formation during the reaction can be expressed as,

$$[\text{product}] = \lim_{n\to\infty} \sum_{i=1}^{n} \alpha^i [\text{enzyme}] \qquad (5)$$

where, α is the proportion of enzyme species that participates in the next catalytic cycle in each turnover while the proportion that is hyperoxidized is represented by $1-\alpha$. Because the value of [product]/[enzyme] finally reached about 2 (Fig. 6B), α was determined to be 0.67 from Eq. 5 under the conditions used in this study. These results indicate that almost one-third of the sulphenic acid intermediate accommodated by Cys-247 is further oxidized to completely inactivate the mutant enzyme at every catalytic cycle, due to the absence of a cysteine sulphinic acid at the position corresponding to Cys-126. These results are consistent with the suggestion that Cys-247 is capable of reacting with H_2O_2, but reacts less so with *t*-BuOOH, under conditions where Cys-126 is not available. Furthermore, it seems most likely that the Cys-126 sulphinic acid, as identified by the LC–MS analysis, protects the alternative catalytic thiol from being inactivated by oxidation.

Discussion

Inactivation based on hyperoxidation of the catalytic cysteine residue has been reported for various 2-Cys type Prxs (*24*, *30*, *31*, *33*, *34*). The inactivation is due

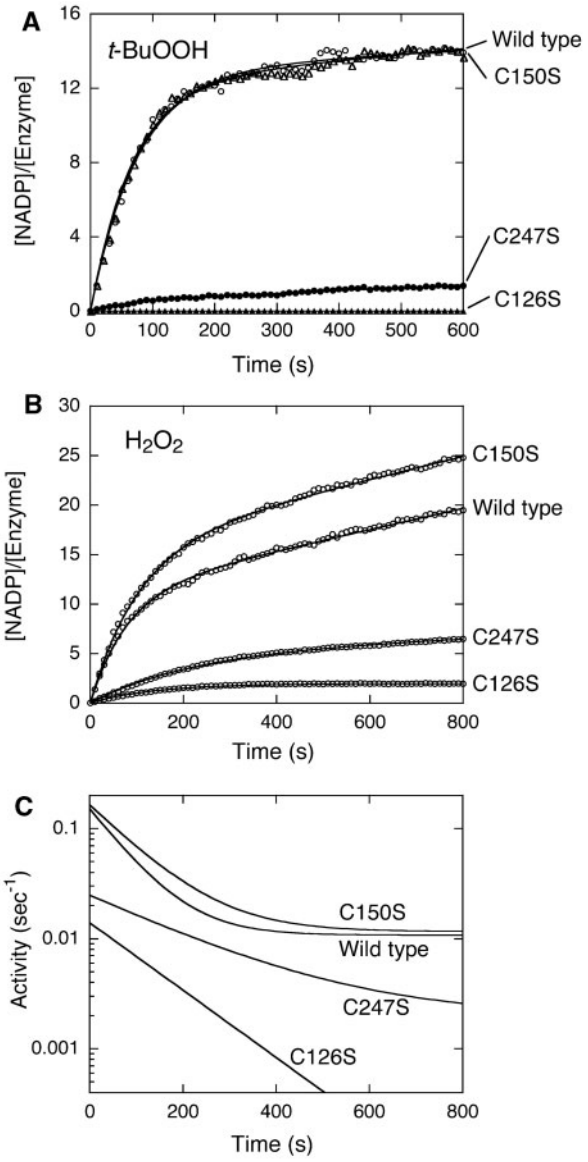

Fig. 6 The reactions of Cys-mutants of Prx-4 with *t*-BuOOH and H_2O_2. (A and B) Time course of NADP production is shown for the wild-type and cysteine-mutants. The data are displayed on a molar basis in order to evaluate the total turnover number for the C126S mutant. Curve fitting was carried out as in Figs 1 and 2. (C) The derivatives of the fitted curves in (B) are shown for reactions with H_2O_2.

to further oxidation of a sulphenic acid intermediate formed at the N-terminal peroxidatic cysteine to sulphinic acid (*24*) or sulphonic acid for some eukaryotic Prxs (*33*, *45*, *46*) by a substrate peroxide. Since the sulphinic acid in the hyperoxidized state is relatively stable and resistant to reduction by Trx, the enzyme is no longer capable of detoxifying peroxides due to unavailability of the catalytic cysteine that plays a primary and central role in attacking the substrate. In this study, we initially observed that H_2O_2 uniquely alters the enzymatic properties of Prx-4 rather than completely inactivating the enzyme, whereas the structural alteration associated with the oxidative damage was not unique but was identified to be the quite ordinary formation of a sulphinic acid at Cys-126, the peroxidatic cysteine residue, as has been reported for a number of other Prx family enzymes. It was then found that the damaged Prx-4 is still capable of detoxifying H_2O_2, but has only a slight activity for *t*-BuOOH, to the significant extent of the intact enzyme. It thus appears that the hyperoxidation of the peroxidatic cysteine leads to a transition into a 'low-activity' form that has a different substrate preference rather than causing a complete loss of activity (Fig. 7).

As indicated by mutational analyses, although Cys-126 is absolutely required for the enzyme to react with *t*-BuOOH, the reaction with H_2O_2 results in the production of NADP by at least two rounds of the catalytic cycle in the absence of a thiol at Cys-126, suggesting that H_2O_2 accesses the other catalytic thiol of Cys-247 and undergoes attack. The bulky nature of *t*-BuOOH could restrict its accessibility to the alternative catalytic thiol group in the active site, while the enzyme might permit the smallest peroxide, H_2O_2 to react with the group. H_2O_2 primarily or predominantly reacts with the Cys-126 residue in the intact form of the enzyme, as revealed by the initial phase where the enzyme retains a higher peroxidase activity (Figs 1 and 2), but can react with Cys-247, in place of Cys-126, when this primary cysteine becomes unavailable due to its hyperoxidation to a sulphinic acid.

The hyperoxidized Prx-4 appeared to detoxify H_2O_2 in a manner dependent on Cys-247 as the alternative catalytic thiol, and no longer underwent further inactivation. On the other hand, the mutant with the Cys-126 replaced, initially displayed the H_2O_2 peroxidase activity to a similar extent to the hyperoxidized wild-type Prx-4, but this activity was not retained (Fig. 6C). The exponential loss of activity can be attributed to irreversible oxidation, which might result from hyperoxidation of the alternative catalytic thiol. Thus, the findings herein suggest that the presence of a cysteine sulphenic acid at Cys-126 confers a protective role against oxidative damage of the alternative catalytic cysteine. In contrast to the case of the mutant, the Cys-126-hyperoxidized enzyme is not able to accept the second H_2O_2 molecule, which is required for the further oxidization of the putative sulphenic acid at Cys-247. Currently, the precise role of the sulphinic acid at Cys-126 in the proposed alternative catalytic mechanism is not known. The enzyme could contain a limited vacancy in close proximity to Cys-247, allowing a H_2O_2 molecule to access this residue but not sufficiently large to accommodate *t*-BuOOH. It is also possible that the highly polarized sulphinic acid group limits the accessibility of relatively hydrophobic peroxide, such as *t*-BuOOH, into the active site. In addition, the sulphinic acid formed at Cys-126 may or may not prohibit the access of a second H_2O_2 and the formation of a neighbouring sulphinic acid, for example, via a possible exclusive interaction and steric hindrance, both of which might be absent in the C126S mutant.

In contrast to an apparent bimolecular reaction for the inactivation by *t*-BuOOH, a saturating kinetic profile unique to the reaction with H_2O_2 may be

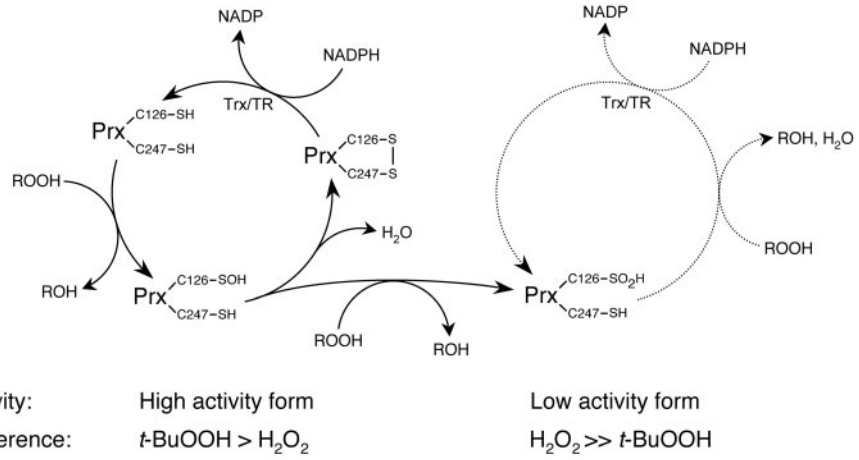

Fig. 7 Schematic representation of the conversion of Prx-4 by reaction with peroxide. The left catalytic cycle is a common mechanism for typical 2-Cys type Prxs (solid line). The right catalytic cycle (dashed line) represents an alternative mechanism, the details of which are described in the text. Hyperoxidation of Prx-4 allows for a transition rather than inactivation. TR denotes Trx reductase.

reasonably explained by a different mechanism in which an additional enzyme species is involved. For example, it is possible that the enzyme species with Cys-126-sulphenic acid forms a non-covalent complex with H_2O_2 with an apparent dissociation constant of 0.12 mM, prior to hyperoxidation. Alternatively, considering the reactivity of Cys-247 with H_2O_2 as discussed above, such an intermediate could be an enzyme species in which two sulphenic acids are formed in both catalytic cysteines, Cys-126 and Cys-247. In this scenario, sulphenic acid formation at Cys-126 is conceivably accompanied by the same modification at Cys-247, and intramolecular but interpeptidyl dismutation would then give rise to the further oxidation of Cys-126 to a sulphinic acid and the restoration of Cys-247 back to a thiol. Other mechanisms are also clearly possible, and why Cys-126 undergoes hyperoxidation by H_2O_2 but not *t*-BuOOH, displaying a saturating kinetic profile, remains to be determined.

Although, it is generally believed that mammalian typical 2-Cys type Prx is inactivated as the result of the loss of the catalytic peroxidatic thiol, our current study found that the hyperoxidized Prx-4 is still active more specifically with respect to H_2O_2. Prx-4 is generally thought to be a secretable ER resident protein (*39*, *40*), and is thought to be associated with disulphide formation, protein folding, ER stress and other types of oxidative stress (*34*, *47*, *48*). It seems evident that the enzyme plays a role in protecting cells from H_2O_2 produced in this organelle. When B cells are differentiated or stimulated by LPS, the expression of this isoform is enhanced (*47*, *49*). Because of the significant remaining peroxidase activity upon the hyperoxidation of Prx-4, the capacity for the detoxification of H_2O_2 by this enzyme can still be counterbalanced by a compensating increase in protein levels. A substantial enhancement in expression, as reported (*47*), may be sufficient for B cells to detoxify H_2O_2 generated accompanying with production of large amounts of antibody, even if the hyperoxidation impairs the enzyme activity by decreasing it to 10%. In addition, after the formation of a sulphinic acid at the peroxidatic cysteine, Prx-4 becomes resistant to further oxidative damage, and, as the result, the enzyme would uniquely serve as a persistent scavenger for H_2O_2. In fact, it has been reported that H_2O_2 is produced at high levels by Ero-1 in the lumen of the ER (*50*), the proposed conversion of Prx-4 seems reasonable in view of the fact that the enzyme plays a role in the detoxification of H_2O_2.

A floodgate hypothesis has been proposed for mammalian and other eukaryotic Prxs, and an inactivation process involving hyperoxidation is considered to be the result of evolution for the regulated flow of H_2O_2 as a cellular signal (*35*, *37*, *38*). However, the findings reported in this study may be somewhat inconsistent with the floodgate model, but Prx-4 could be further adapted to allow the persistent breakdown of H_2O_2 or a constant transfer of reducing equivalents for oxidative folding processes in the ER of secretory cells (*49*).

Conflict of interest
None declared.

References

1. Kim, K., Kim, I.H., Lee, K.Y., Rhee, S.G., and Stadtman, E.R. (1988) The isolation and purification of a specific "protector" protein which inhibits enzyme inactivation by a thiol/Fe(III)/O2 mixed-function oxidation system. *J. Biol. Chem.* **263**, 4704–4711
2. Chae, H.Z., Robison, K., Poole, L.B., Church, G., Storz, G., and Rhee, S.G. (1994) Cloning and sequencing of thiol-specific antioxidant from mammalian brain: alkyl hydroperoxide reductase and thiol-specific antioxidant define a large family of antioxidant enzymes. *Proc. Natl. Acad. Sci. USA* **91**, 7017–7021
3. Chae, H.Z., Kim, H.J., Kang, S.W., and Rhee, S.G. (1999) Characterization of three isoforms of mammalian peroxiredoxin that reduce peroxides in the presence of thioredoxin. *Diabetes Res. Clin. Pract.* **45**, 101–112
4. Chae, H.Z., Kang, S.W., and Rhee, S.G. (1999) Isoforms of mammalian peroxiredoxin that reduce peroxides in presence of thioredoxin. *Methods Enzymol.* **300**, 219–226

5. Chae, H.Z., Chung, S.J., and Rhee, S.G. (1994) Thioredoxin-dependent peroxide reductase from yeast. *J. Biol. Chem.* **269**, 27670–27678
6. Rhee, S.G., Kang, S.W., Chang, T.S., Jeong, W., and Kim, K. (2001) Peroxiredoxin, a novel family of peroxidases. *IUBMB Life* **52**, 35–41
7. Fujii, J. and Ikeda, Y. (2002) Advances in our understanding of peroxiredoxin, a multifunctional, mammalian redox protein. *Redox Rep.* **7**, 123–130
8. Ishii, T., Itoh, K., Akasaka, J., Yanagawa, T., Takahashi, S., Yoshida, H., Bannai, S., and Yamamoto, M. (2000) Induction of murine intestinal and hepatic peroxiredoxin MSP23 by dietary butylated hydroxyanisole. *Carcinogenesis* **21**, 1013–1016
9. Furuta, J., Nobeyama, Y., Umebayashi, Y., Otsuka, F., Kikuchi, K., and Ushijima, T. (2006) Silencing of Peroxiredoxin 2 and aberrant methylation of 33 CpG islands in putative promoter regions in human malignant melanomas. *Cancer Res.* **66**, 6080–6086
10. Chang, X.Z., Li, D.Q., Hou, Y.F., Wu, J., Lu, J.S., Di, G.H., Jin, W., Ou, Z.L., Shen, Z.Z., and Shao, Z.M. (2007) Identification of the functional role of peroxiredoxin 6 in the progression of breast cancer. *Breast Cancer Res.* **9**, R76
11. Iraqui, I., Faye, G., Ragu, S., Masurel-Heneman, A., Kolodner, R.D., and Huang, M.E. (2008) Human peroxiredoxin PrxI is an orthologue of yeast Tsa1, capable of suppressing genome instability in Saccharomyces cerevisiae. *Cancer Res.* **68**, 1055–1063
12. Song, I.S., Kim, S.U., Oh, N.S., Kim, J., Yu, D.Y, Huang, S.M., Kim, J.M., Lee, D.S., and Kim, N.S. (2009) Peroxiredoxin I contributes to TRAIL resistance through suppression ofredox-sensitive caspase activation in human hepatoma cells. *Carcinogenesis* **30**, 1106–1114
13. Neumann, C.A., Krause, D.S., Carman, C.V., Das, S., Dubey, D.P., Abraham, J.L., Bronson, R.T., Fujiwara, Y., Orkin, S.H., and Van Etten, R.A. (2003) Essential role for the peroxiredoxin Prdx1 in erythrocyte antioxidant defence and tumour suppression. *Nature* **424**, 561–565
14. Demasi, A.P., Ceratti, D., Furuse, C., Cury, P., Junqueira, J.L., and Araujo, V.C. (2007) Expression of peroxiredoxin I in plasma cells of oral inflammatory diseases. *Eur. J. Oral Sci.* **115**, 334–337
15. Yang, C.S., Lee, D.S., Song, C.H., An, S.J., Li, S., Kim, J.M., Kim, C.S., Yoo, D.G., Jeon, B.H., Yang, H.Y., Lee, T.H., Lee, Z.W., El-Benna, J., Yu, D.Y., and Jo, E.K. (2007) Roles of peroxiredoxin II in the regulation of proinflammatory responses to LPS and protection against endotoxin-induced lethal shock. *J. Exp. Med.* **204**, 583–594
16. Li, L., Shoji, W., Takano, H., Nishimura, N., Aoki, Y., Takahashi, R., Goto, S., Kaifu, T., Takai, T., and Obinata, M. (2007) Increased susceptibility of MER5 (peroxiredoxin III) knockout mice to LPS-induced oxidative stress. *Biochem. Biophys. Res. Commun.* **355**, 715–721
17. Fang, J., Nakamura, T., Cho, D.H., Gu, Z., and Lipton, S.A. (2007) S-nitrosylation of peroxiredoxin 2 promotes oxidative stress-induced neuronal cell death in Parkinson's disease. *Proc. Natl. Acad. Sci. USA* **104**, 18742–18747
18. Yao, J., Taylor, M., Davey, F., Ren, Y., Aiton, J., Coote, P., Fang, F., Chen, J.X., Yan, S.D., and Gunn-Moore, F.J. (2007) Interaction of amyloid binding alcohol dehydrogenase/Abeta mediates up-regulation of peroxiredoxin II in the brains of Alzheimer's disease patients and a transgenic Alzheimer's disease mouse model. *Mol. Cell. Neurosci.* **35**, 377–382
19. Qu, D., Rashidian, J., Mount, M.P., Aleyasin, H., Parsanejad, M., Lira, A., Haque, E., Zhang, Y., Callaghan, S., Daigle, M., Rousseaux, M.W., Slack, R.S., Albert, P.R., Vincent, I., and Woulfe, J.M. (2007) D.S. Park, Role of Cdk5-mediated phosphorylation of Prx2 in MPTP toxicity and Parkinson's disease. *Neuron* **55**, 37–52
20. Chae, H.Z., Uhm, T.B., and Rhee, S.G. (1994) Dimerization of thiol-specific antioxidant and the essential role of cysteine 47. *Proc. Natl. Acad. Sci. USA* **91**, 7022–7026
21. Wood, Z.A., Schroder, E., Robin Harris, J., and Poole, L.B. (2003) Structure, mechanism and regulation of peroxiredoxins. *Trends Biochem. Sci.* **28**, 32–40
22. Watabe, S., Kohno, H., Kouyama, H., Hiroi, T., Yago, N., and Nakazawa, T. (1994) Purification and characterization of a substrate protein for mitochondrial ATP-dependent protease in bovine adrenal cortex. *J. Biochem.* **115**, 648–654
23. Mitsumoto, A., Takanezawa, Y., Okawa, K., Iwamatsu, A., and Nakagawa, Y. (2001) Variants of peroxiredoxins expression in response to hydroperoxide stress. *Free Radic. Biol. Med.* **30**, 625–635
24. Yang, K.S., Kang, S.W., Woo, H.A., Hwang, S.C., Chae, H.Z., Kim, K., and Rhee, S.G. (2002) Inactivation of human peroxiredoxin I during catalysis as the result of the oxidation of the catalytic site cysteine to cysteine-sulfinic acid. *J. Biol. Chem.* **277**, 38029–38036
25. Biteau, B., Labarre, J., and Toledano, M.B. (2003) ATP-dependent reduction of cysteine-sulphinic acid by S. cerevisiae sulphiredoxin. *Nature* **425**, 980–984
26. Chang, T.S., Jeong, W., Woo, H.A., Lee, S.M., Park, S., and Rhee, S.G. (2004) Characterization of mammalian sulfiredoxin and its reactivation of hyperoxidized peroxiredoxin through reduction of cysteine sulfinic acid in the active site to cysteine. *J. Biol. Chem.* **279**, 50994–51001
27. Rhee, S.G., Kang, S.W., Jeong, W., Chang, T.S., Yang, K.S., and Woo, H.A. (2005) Intracellular messenger function of hydrogen peroxide and its regulation by peroxiredoxins. *Curr. Opin. Cell. Biol.* **17**, 183–189
28. Jonsson, T.J., Johnson, L.C., and Lowther, W.T. (2008) Structure of the sulphiredoxin–peroxiredoxin complex reveals an essential repair embrace. *Nature* **451**, 98–101
29. Woo, H.A., Chae, H.Z., Hwang, S.C., Yang, K.S., Kang, S.W., Kim, K., and Rhee, S.G. (2003) Reversing the inactivation of peroxiredoxins caused by cysteine sulfinic acid formation. *Science* **300**, 653–656
30. Cox, A.G., Pearson, A.G., Pullar, J.M., Jonsson, T.J., Lowther, W.T., Winterbourn, C.C., and Hampton, M.B. (2009) Mitochondrial peroxiredoxin 3 is more resilient to hyperoxidation than cytoplasmic peroxiredoxins. *Biochem. J.* **421**, 51–58
31. Bae, S.H., Woo, H.A., Sung, S.H., Lee, H.E., Lee, S.K., Kil, I.S., and Rhee, S.G. (2009) Induction of sulfiredoxin via an Nrf2-dependent pathway and hyperoxidation of peroxiredoxin III in the lungs of mice exposed to hyperoxia. *Antioxid. Redox Signal.* **11**, 937–948
32. Kim, S.Y., Jo, H.Y., Kim, M.H., Cha, Y.Y., Choi, S.W., Shim, J.H., Kim, T.J., and Lee, K.Y. (2008) H_2O_2-dependent hyperoxidation of peroxiredoxin 6 (Prdx6) plays a role in cellular toxicity via up-regulation of iPLA2 activity. *J. Biol. Chem.* **283**, 33563–33568
33. Moon, J.C., Hah, Y.S., Kim, W.Y., Jung, B.G., Jang, H.H., Lee, J.R., Kim, S.Y., Lee, Y.M., Jeon, M.G., Kim, C.W., Cho, M.J., and Lee, S.Y. (2005) Oxidative stress-dependent structural and functional switching of a human 2-Cys peroxiredoxin isotype II that enhances HeLa cell resistance to H_2O_2-induced cell death. *J. Biol. Chem.* **280**, 28775–28784

34. Tavender, T.J. and Bulleid, N.J. (2010) Peroxiredoxin IV protects cells from oxidative stress by removing H_2O_2 produced during disulphide formation. *J. Cell Sci.* **123**, 2672–2679
35. Wood, Z.A., Poole, L.B., and Karplus, P.A. (2003) Peroxiredoxin evolution and the regulation of hydrogen peroxide signaling. *Science* **300**, 650–653
36. Rhee, S.G. (2006) Cell signaling. H_2O_2, a necessary evil for cell signaling. *Science* **312**, 1882–1883
37. Jara, M., Vivancos, A.P., and Hidalgo, E. (2008) C-terminal truncation of the peroxiredoxin Tpx1 decreases its sensitivity for hydrogen peroxide without compromising its role in signal transduction. *Genes Cells* **13**, 171–179
38. Koo, K.H., Lee, S., Jeong, S.Y., Kim, E.T., Kim, H.J., Kim, K., Song, K., and Chae, H.Z. (2002) Regulation of thioredoxin peroxidase activity by C-terminal truncation. *Arch. Biochem. Biophys.* **397**, 312–318
39. Okado-Matsumoto, A., Matsumoto, A., Fujii, J., and Taniguchi, N. (2000) Peroxiredoxin IV is a secretable protein with heparin-binding properties under reduced conditions. *J. Biochem.* **127**, 493–501
40. Tavender, T.J., Sheppard, A.M., and Bulleid, N.J. (2008) Peroxiredoxin IV is an endoplasmic reticulum-localized enzyme forming oligomeric complexes in human cells. *Biochem. J.* **411**, 191–199
41. Ikeda, Y., Ito, R., Ihara, H., Okada, T., and Fujii, J. (2010) Expression of N-terminally truncated forms of rat peroxiredoxin-4 in insect cells. *Protein Expr. Purif.* **72**, 1–7
42. Matsumoto, A., Okado, A., Fujii, T., Fujii, J., Egashira, M., Niikawa, N., and Taniguchi, N. (1999) Cloning of the peroxiredoxin gene family in rats and characterization of the fourth member. *FEBS Lett.* **443**, 246–250
43. Laemmli, U.K. (1970) Cleavage of structural proteins during the assembly of the head of bacteriophage T4. *Nature* **227**, 680–685
44. Manta, B., Hugo, M., Ortiz, C., Ferrer-Sueta, G., Trujillo, M., and Denicola, A. (2009) The peroxidase and peroxynitrite reductase activity of human erythrocyte peroxiredoxin 2. *Arch. Biochem. Biophys.* **484**, 146–154
45. Lee, C.K., Kim, H.J., Lee, Y.R., So, H.H., Park, H.J., Won, K.J., Park, T., Lee, K.Y., Lee, H.M., and Kim, B. (2007) Analysis of peroxiredoxin decreasing oxidative stress in hypertensive aortic smooth muscle. *Biochim. Biophys. Acta* **1774**, 848–855
46. Lim, J.C., Choi, H.I., Park, Y.S., Nam, H.W., Woo, H.A., Kwon, K.S., Kim, Y.S., Rhee, S.G., Kim, K., and Chae, H.Z. (2008) Irreversible oxidation of the active-site cysteine of peroxiredoxin to cysteine sulfonic acid for enhanced molecular chaperone activity. *J. Biol. Chem.* **283**, 28873–28880
47. Bertolotti, M., Yim, S.H., Garcia-Manteiga, J.M., Masciarelli, S., Kim, Y.J., Kang, M.H., Iuchi, Y., Fujii, J., Vene, R., Rubartelli, A., Rhee, S.G., and Sitia, R. (2010) B- to plasma-cell terminal differentiation entails oxidative stress and profound reshaping of the antioxidant responses. *Antioxid. Redox Signal.* **13**, 1133–1144
48. Iuchi, Y., Okada, F., Tsunoda, S., Kibe, N., Shirasawa, N., Ikawa, M., Okabe, M., Ikeda, Y., and Fujii, J. (2009) Peroxiredoxin 4 knockout results in elevated spermatogenic cell death via oxidative stress. *Biochem. J.* **419**, 149–158
49. van Anken, E., Romijn, E.P., Maggioni, C., Mezghrani, A., Sitia, R., Braakman, I., and Heck, A.J. (2003) Sequential waves of functionally related proteins are expressed when B cells prepare for antibody secretion. *Immunity* **18**, 243–253
50. Enyedi, B., Varnai, P., and Geiszt, M. (2010) Redox state of the endoplasmic reticulum is controlled by Ero1L-alpha and intraluminal calcium. *Antioxid. Redox Signal.* **13**, 721–729